Parametric analysis of the three-column spar platform for 6MW offshore wind turbine

Paweł Dymarski, Ewelina Ciba
Gdansk University of Technology, Gdansk/Poland
pawdymar@pg.edu.pl

1 Introduction

The dynamic development of the offshore wind energy sector in such countries as UK, Germany, Denmark, Netherlands means that shallow water areas are exhausted (with a depth of 40-50m), therefore wind farm projects at a depth of 50m+ are considered. In 2017, the first floating (deep water) mini-farm "Hywind" was launched off the coast of Scotland.

The "Hywind Scotland" farm is located on a 105 m deep water reservoir. The draft of a single platform is 78 meters. The anchoring system is of catenary type - steel chains are attached to suction piles. Each pile is about 15 meters high.

The main aim of this work was to develop an innovative concept of a three-column spar floating platform for a 6MW wind turbine for Polish Exclusive Economic Zone for 65m+ moderate water depth reservoirs. The key issues related to the use of floating platforms as supporting structures are the stability of platforms and the dynamic behavior of these platforms on the wave.

The authors present the stability analysis of the platform for various sizes of cylindrical buoyancy tanks and using different types of ballast. The authors investigated the influence of these parameters on the trim angle of the platform due to the thrust load on the turbine. Based on the results of parametric analysis and based on specific stability criteria, geometrical models of selected variants were created.

For these solutions, a preliminary analysis of platform dynamics was carried out in the conditions of a 50-year storm. Based on calculations of platform on the wave (using a simplified model), the amplitudes of platform motions, the maximum values of tendons tensions resulting from environmental forces were determined.

2 General types of floating wind turbines

Floating offshore wind turbines can be divided into three types due to the method of obtaining stability: tension leg platforms (mooring lines stabilized platforms), semisubmersible platforms (buoyancy stabilized platforms) and spar platforms (ballast stabilized platforms).

Spar platforms are also divided into the following concepts [1]:

- *"Classic" spar* - the hull of the platform is a cylinder, in the lower part there is a ballast, the upper, usually larger, part of the cylinder is empty,
- *truss spar* - the hull of the platform consists of two separate parts: a large buoyancy tank (at the top) and a small ballast tank located at the bottom of the platform. The tanks are connected by a lattice structure with a height of about half of the platform's draft.
- *Cell spar* - the hull is made up of seven cylinders (usually with the same diameter), three cylinders are significantly longer than the others, they keep the ballast tank in the bottom of the platform.

In this work, the third of the types of floating platforms has been developed. The concept of the three-column spar platform is presented in Fig. 1. The platform consists of three columns with a larger diameter around the waterline and a smaller one in the more submerged part. Cylindrical parts are connected with each other by conical elements. Cylinders are connected to each other at the top (above the water line) where there is a "deck" to which the tower is mounted and at the bottom where the ballast tank is located. The additional connection is located at the height of the attachment points of the tendons, this connection is to align the distribution of forces between the columns due to the reaction force from the anchoring system.

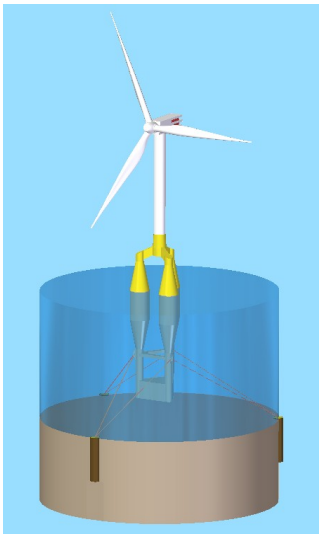

Fig. 1 Three-column spar concept

3 Parametric analysis of static stability

The main goal of the parametric analysis is to assess the static stability of the platform as a function of the two parameters:

- the diameter of the upper cylinders D_{tank} (change of buoyancy),
- the density of the ballast $\rho_{ballast}$, which is placed in the "triangular" bottom tank.The range of the upper cylinder diameter is: D_{tank} = 10 – 12 m, however, the assumed range of ballast density is: $\rho_{ballast}$ = 2600 – 4600 kg/m^3.

The lower value of ballast density corresponds to the density of concrete, while the upper value of the ballast density is close to the density of iron ore.

Static stability analysis of the platform consisted in calculating the trim angle due to the aerodynamic thrust force on the turbine. The desired value of the trim angle is the smallest value. It was assumed, however, that the trim with a value of θ=6˚is acceptable. The maximum static thrust on the turbine is T = 800kN [2, 3]. The value of thrust includes the impact of wind on the platform's tower.

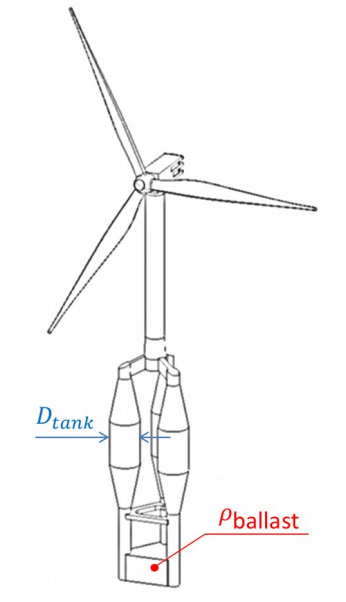

Fig. 2 Parameters D_{tank} and $\rho_{ballast}$

The graph (Fig. 4) show the obtained trim angles θ on the effects of the static thrust force T=800kN for a given range of parameters D_{tank} and $\rho_{ballast}$. On the basis of obtained values of the trim angle as a function of parameters D_{tank} and $\rho_{ballast}$, the area of feasible solutions was determined due to the trim θ caused by the thrust force.

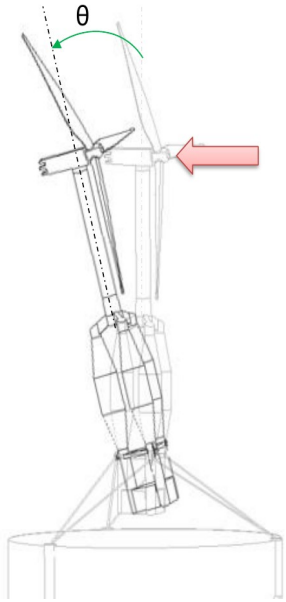

Fig. 3 Trim angle due to thrust force.

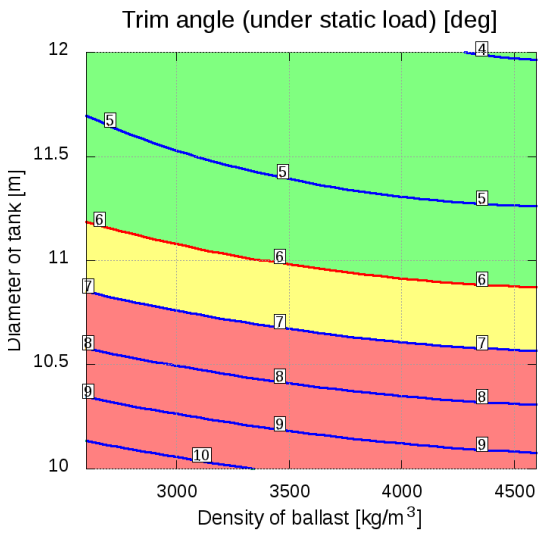

Fig. 4 Trim angle as a function of parameters D_{tank} and $\rho_{ballast}$. Green colour indicates the area of permissible parameters based on the limit line of the trim angle θ_c=6 ˚.

4 Analysis of platform dynamics

The second goal of the parametric analysis is to evaluate the amplitudes of platform movements in the function of the these parameters.

It is particularly important to analyse the heave and pitch motion of the platform. Minimizing horizontal movements (heave) is important due to the limited depth of the basin, the platform can not hit the bottom of the sea. Vertical accelerations, on the other hand, increase the loads from the mass of the structure.

4.1 Hydro-meteorological condition

The analysis of the movement of the platform subjected to wind, wave and sea currents was made for survival conditions [4]:

- Significant wave height: H_s=9m, peak period: T_p=11.3s, speed of sea current U_{curr} =0.45m/s
- Mean wind speed at the height of 10 meters: $U_{w,H=10m}$ = 29.1m/s.

The above weather conditions correspond to the conditions of a 50-year storm (recommended by classification societies [5]). The turbine is turned off.

The wave spectrum was approximated using JONSWAP formula, however the non-stationary character of wind speed was modelled using Ochi-Shin spectrum [6].

In order to disturb the symmetry of external forces, it was assumed that the wind direction is deviated from the wave direction by 10 degrees. This approach results in the fact that the platform is moving in six degrees of freedom, which allows to observe additional (often negative) effects.

4.2 Computational model

The computational model is based on the generalized Morison equation. The structure - consisting mainly of cylindrical elements - has been divided into segments. For each segment, forces are calculated using local velocity and water acceleration values as well as local velocity and acceleration of a given part of the structure. The thrust force on the turbine is calculated based on the thrust coefficient (which is constant for given conditions).

The vector of hydrodynamic force on the i-th cylindical segment is calculated using the formula [7, 8]:

$$\boldsymbol{F}_i = \frac{1}{2} C_D \rho A_{p,i} \left| \boldsymbol{u}_{n,i} - \dot{\boldsymbol{x}}_{n,i} \right| \left(\boldsymbol{u}_{n,i} - \dot{\boldsymbol{x}}_{n,i} \right) + \rho V_{b,i} \left(1 + C_A \right) \dot{\boldsymbol{u}}_{n,i} - \rho V_{b,i} C_A \ddot{\boldsymbol{x}}_{n,i} \quad , \tag{1}$$

where C_D – drag coefficient in the direction normal to the cyliner axis; ρ – water density; $A_{p,i}$ – projection of the segment surface onto the direction normal to the cylinder axis; $\boldsymbol{u}_{n,i}$, $\dot{\boldsymbol{u}}_{n,i}$ - water velocity and acceleration component normal to the cylinder axis, $V_{b,i}$ - segment volume, C_A – added mass coefficient, $\dot{\boldsymbol{x}}_{n,i}$, $\ddot{\boldsymbol{x}}_{n,i}$ – component of velocity and acceleration of the segment normal to the cylinder axisin.
The thrust force on the turbine is calculated from the following formula:

$$T = C_T \frac{1}{2} \rho_{air} A_T \left| u_w - u_t \right| \left(u_w - u_t \right) \quad , \tag{2}$$

where C_T – thrust coefficient of rotor, A_T – area of the rotor disk, ρ_{air} – air density, u_w – wind speed, u_t – the speed of the turbine hub.
The forces of the anchoring system are determined based on the characteristics of force F_t - elongation ε_t of tendons [9]. The actual tendon characteristics are shown in Fig. 5, for the purposes of the calculations the characteristics described in the 5th degree polynomial were adopted. Platform movement is calculated in six degrees of freedom with the assumption that the structure is rigid.
The breaking force of the rope is $F_{breaking}$=12 MN.

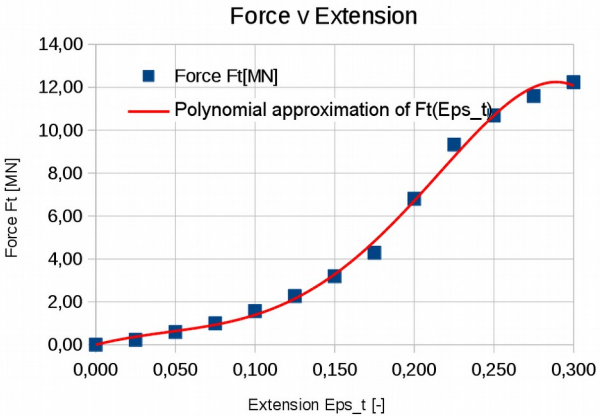

Fig. 5 Polynomial characteristics F_t vs ε_t of tendons. Rope: "*VIKING BRAIDLINE Nylon*", D_{rope}=240mm

4.3 Computation results

As the results of the wave motion calculations of the platform, we obtain graphs: surge, sway and heave motion as a function of time (Fig. 6 a). The horizontal acceleration of the nacelle, which is the main cause of the tower load is shown in Fig. 6 b), angular motions are shown in Fig. 6 c) and force in the ropes of the anchoring system are shown in Fig. 6 d). The results relate to the case: D_{tank} = 11m, $\rho_{ballast}$ = 3600 kg/m^3.

On the basis of the results of calculations in the time domain, diagrams of maximum values of heave amplitude, amplitude of nacelle acceleration, pitch and values of maximum forces in the tendons were created (Fig. 7 a, b, c, d). These diagrams were prepared in the field of D_{tank} and $\rho_{ballast}$ parameters.The area of acceptable values (of a given quantity) is marked with green, yellow indicates values at a critical level, which, however, can still be considered as acceptable. The areas in which the given values exceed the critical values are marked in red.

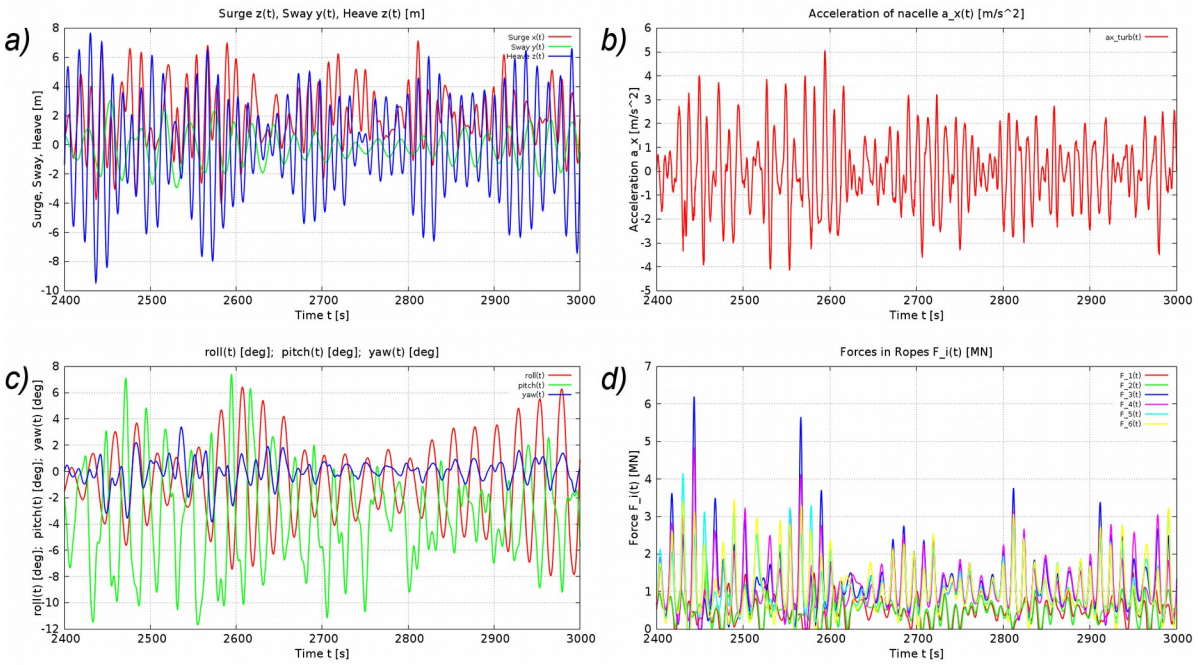

Fig. 6 a) Linear motions: surge (red), sway (green), heave (blue); b) linear, horizontal accelerations of nacelle Forces in ropes; c) Angular motions: roll (red), pitch (green), yaw (blue); d) Forces in ropes. The graphs show results for 600 seconds. The total simulation time is 3 hours (10800 seconds)

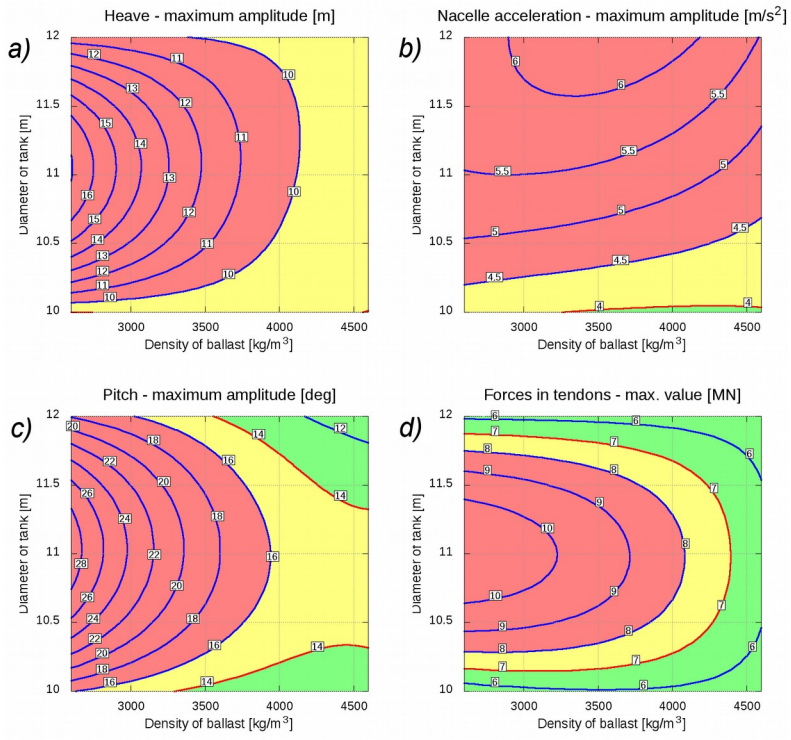

Fig. 7 Diagrams of maximum values recorded during a simulation lasting 3 hours: **a)** heave amplitude; **b)** acceleration amplitude; **c)** pitch amplitude; **d)** the maximum values of forces in the tendons

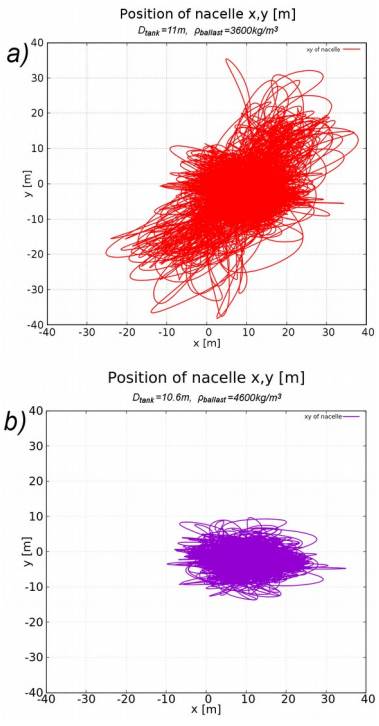

Fig. 8 Path of nacelle *x,y* (top view): **a)** variant from the middle of parametric area: D_{tank}=11m, $\rho_{ballast}$=3600kg/m^3; **b)** Acceptable solution D_{tank}=10.6m, $\rho_{ballast}$=4600kg/m^3

4 Conclusions and comments

- Based on the hydrostatic analysis for the design wind conditions, the trim angle θ was determined as a function of D_{tank} and $\rho_{ballast}$ parameters (Fig. 4). The chart shows that as the diameter of the displacement tanks D_{tank} increases, the trim angle decreases, which for the given range of parameters is between 4 and 10.5 degrees. It is noteworthy that a change in ballast density ρ_{ballas} (and a change in ballast tank size) has little effect on the trim angle achieved.
- The analysis of the calculations results of platform dynamics on the wave shows that the biggest problem are the large values of horizontal acceleration of the nacelle, which are the main reason for the bending moments of the platform's central column (tower). Assuming that the limit value of horizontal acceleration is $a_{x,nacelle,c}$=4.0 m/s^2 (Fig. 7 b), we obtain an area of permissible values that does not coincide with the area of the permissible trim angle, Fig. 4 (see item above). There is no acceptable solution.
- Loosening the criterion of maximum horizontal accelerations in such a way that we assume a critical value of $a_{x,nacelle,c}$=4.5 m/s^2 with a simultaneous increase of the minimum (critical) trim angle to the value of θ_c=7° will cause that the area of solutions acceptable in the small surroundings of the point D_{tank}=10.6 m, $\rho_{ballast}$=4600 kg/m^3 will appear. Fig. 8 shows the comparison between path (trajectory) of nacelle for case D_{tank}=11m, $\rho_{ballast}$=3600kg/m^3 (the middle of parametric area) and path of nacelle motion for the acceptable solution. The smaller the size of the "cloud", the better the conditions for turbine operation
- The authors' experience shows that the amplitudes of movements predicted using CFD, as well as the predicted amplitudes based on model tests are smaller than the amplitudes of motions obtained using a model based on the Morison equation. Probably the real area of acceptable solutions is larger than obtained in this paper.

Acknowledgement

This research was supported by The Polish National Centre for Research and Development (NCBR) under the project “WIND-TU-PLA” ERA-NET MARTEC II (Agreement No. MARTECII/1/2014).

References

[1] Moo-Hyun Kim (2012). SPAR Platforms. Technology and Analysis Methods. American Society of Civil Engineers

[2] Jonkman J., Butterfield S., Musial W., Scott G. (2009). Definition of a 5-MW Reference Wind Turbine for Offshore System Development. National Renewable Energy Laboratory, Technical Report NREL/TP-500-38060 February 2009

[3] Kooijman H.J.T., Lindenburg C., Winkelaar D., van der Hooft E.L. (2003). DOWEC 6 MW PRE-DESIGN. Aero-elastic modelling of the DOWEC 6 MW pre-design in PHATAS. Report DOWEC-F1W2-HJK-01-046/9 (public version). September 2003

[4] Dymarski P., Ciba E., Marcinkowski T. (2016). Effective method for determining environmental loads on supporting structures for offshore wind turbines. Polish Maritime Research 23(1(89)), 52-60. https://doi.org/10.1515/pomr-2016-0008

[5] DNVGL-ST-0437 (November 2016) Loads and site conditions for wind turbines

[6] Feikema G.J.,Withers J.E.W. (1991). The Effect of Wind Spectra on the Low-Frequency Motions of a Moored Tanker in Survival Condition. 23rd Annual Offshore Technology Conference in Houston, Texas. May 6-9, 1991

[7] Sarpkaya T. (2010) Wave Forces on Offshore Structures. Cambridge University Press, New York, 2010

[8] Żywicki J., Dymarski P., Ciba E., Dymarski C. (2017). Design of Structure of Tension Leg Platform for 6 MW Offshore Wind Turbine Based On Fem Analysis. Polish Maritime Research 24(s1), 230-241. https://doi.org/10.1515/pomr-2017-0043

[9] BRIDON. Fibre Rope Catalogue